



BELLE-CONF-0413
ICHEP Abstract 11-0658

Observation of $B^+ \rightarrow p\bar{\Lambda}\gamma$

K. Abe,¹⁰ K. Abe,⁴⁶ N. Abe,⁴⁹ I. Adachi,¹⁰ H. Aihara,⁴⁸ M. Akatsu,²⁴ Y. Asano,⁵³
T. Aso,⁵² V. Aulchenko,² T. Aushev,¹⁴ T. Aziz,⁴⁴ S. Bahinipati,⁶ A. M. Bakich,⁴³
Y. Ban,³⁶ M. Barbero,⁹ A. Bay,²⁰ I. Bedny,² U. Bitenc,¹⁵ I. Bizjak,¹⁵ S. Blyth,²⁹
A. Bondar,² A. Bozek,³⁰ M. Bračko,^{22,15} J. Brodzicka,³⁰ T. E. Browder,⁹ M.-C. Chang,²⁹
P. Chang,²⁹ Y. Chao,²⁹ A. Chen,²⁶ K.-F. Chen,²⁹ W. T. Chen,²⁶ B. G. Cheon,⁴
R. Chistov,¹⁴ S.-K. Choi,⁸ Y. Choi,⁴² Y. K. Choi,⁴² A. Chuvikov,³⁷ S. Cole,⁴³
M. Danilov,¹⁴ M. Dash,⁵⁵ L. Y. Dong,¹² R. Dowd,²³ J. Dragic,²³ A. Drutskoy,⁶
S. Eidelman,² Y. Enari,²⁴ D. Epifanov,² C. W. Everton,²³ F. Fang,⁹ S. Fratina,¹⁵
H. Fujii,¹⁰ N. Gabyshev,² A. Garmash,³⁷ T. Gershon,¹⁰ A. Go,²⁶ G. Gokhroo,⁴⁴
B. Golob,^{21,15} M. Grosse Perdekamp,³⁸ H. Guler,⁹ J. Haba,¹⁰ F. Handa,⁴⁷ K. Hara,¹⁰
T. Hara,³⁴ N. C. Hastings,¹⁰ K. Hasuko,³⁸ K. Hayasaka,²⁴ H. Hayashii,²⁵ M. Hazumi,¹⁰
E. M. Heenan,²³ I. Higuchi,⁴⁷ T. Higuchi,¹⁰ L. Hinz,²⁰ T. Hojo,³⁴ T. Hokuue,²⁴
Y. Hoshi,⁴⁶ K. Hoshina,⁵¹ S. Hou,²⁶ W.-S. Hou,²⁹ Y. B. Hsiung,²⁹ H.-C. Huang,²⁹
T. Igaki,²⁴ Y. Igarashi,¹⁰ T. Iijima,²⁴ A. Imoto,²⁵ K. Inami,²⁴ A. Ishikawa,¹⁰ H. Ishino,⁴⁹
K. Itoh,⁴⁸ R. Itoh,¹⁰ M. Iwamoto,³ M. Iwasaki,⁴⁸ Y. Iwasaki,¹⁰ R. Kagan,¹⁴ H. Kakuno,⁴⁸
J. H. Kang,⁵⁶ J. S. Kang,¹⁷ P. Kapusta,³⁰ S. U. Kataoka,²⁵ N. Katayama,¹⁰ H. Kawai,³
H. Kawai,⁴⁸ Y. Kawakami,²⁴ N. Kawamura,¹ T. Kawasaki,³² N. Kent,⁹ H. R. Khan,⁴⁹
A. Kibayashi,⁴⁹ H. Kichimi,¹⁰ H. J. Kim,¹⁹ H. O. Kim,⁴² Hyunwoo Kim,¹⁷ J. H. Kim,⁴²
S. K. Kim,⁴¹ T. H. Kim,⁵⁶ K. Kinoshita,⁶ P. Koppenburg,¹⁰ S. Korpar,^{22,15} P. Križan,^{21,15}
P. Krokovny,² R. Kulasiri,⁶ C. C. Kuo,²⁶ H. Kurashiro,⁴⁹ E. Kurihara,³ A. Kusaka,⁴⁸
A. Kuzmin,² Y.-J. Kwon,⁵⁶ J. S. Lange,⁷ G. Leder,¹³ S. E. Lee,⁴¹ S. H. Lee,⁴¹
Y.-J. Lee,²⁹ T. Lesiak,³⁰ J. Li,⁴⁰ A. Limosani,²³ S.-W. Lin,²⁹ D. Liventsev,¹⁴

J. MacNaughton,¹³ G. Majumder,⁴⁴ F. Mandl,¹³ D. Marlow,³⁷ T. Matsuishi,²⁴
 H. Matsumoto,³² S. Matsumoto,⁵ T. Matsumoto,⁵⁰ A. Matyja,³⁰ Y. Mikami,⁴⁷
 W. Mitaroff,¹³ K. Miyabayashi,²⁵ Y. Miyabayashi,²⁴ H. Miyake,³⁴ H. Miyata,³² R. Mizuk,¹⁴
 D. Mohapatra,⁵⁵ G. R. Moloney,²³ G. F. Moorhead,²³ T. Mori,⁴⁹ A. Murakami,³⁹
 T. Nagamine,⁴⁷ Y. Nagasaka,¹¹ T. Nakadaira,⁴⁸ I. Nakamura,¹⁰ E. Nakano,³³ M. Nakao,¹⁰
 H. Nakazawa,¹⁰ Z. Natkaniec,³⁰ K. Neichi,⁴⁶ S. Nishida,¹⁰ O. Nitoh,⁵¹ S. Noguchi,²⁵
 T. Nozaki,¹⁰ A. Ogawa,³⁸ S. Ogawa,⁴⁵ T. Ohshima,²⁴ T. Okabe,²⁴ S. Okuno,¹⁶
 S. L. Olsen,⁹ Y. Onuki,³² W. Ostrowicz,³⁰ H. Ozaki,¹⁰ P. Pakhlov,¹⁴ H. Palka,³⁰
 C. W. Park,⁴² H. Park,¹⁹ K. S. Park,⁴² N. Parslow,⁴³ L. S. Peak,⁴³ M. Pernicka,¹³
 J.-P. Perroud,²⁰ M. Peters,⁹ L. E. Piilonen,⁵⁵ A. Poluektov,² F. J. Ronga,¹⁰ N. Root,²
 M. Rozanska,³⁰ H. Sagawa,¹⁰ M. Saigo,⁴⁷ S. Saitoh,¹⁰ Y. Sakai,¹⁰ H. Sakamoto,¹⁸
 T. R. Sarangi,¹⁰ M. Satapathy,⁵⁴ N. Sato,²⁴ O. Schneider,²⁰ J. Schümann,²⁹ C. Schwanda,¹³
 A. J. Schwartz,⁶ T. Seki,⁵⁰ S. Semenov,¹⁴ K. Senyo,²⁴ Y. Settai,⁵ R. Seuster,⁹
 M. E. Sevier,²³ T. Shibata,³² H. Shibuya,⁴⁵ B. Shwartz,² V. Sidorov,² V. Siegle,³⁸
 J. B. Singh,³⁵ A. Somov,⁶ N. Soni,³⁵ R. Stamen,¹⁰ S. Stanič,^{53,*} M. Starič,¹⁵ A. Sugi,²⁴
 A. Sugiyama,³⁹ K. Sumisawa,³⁴ T. Sumiyoshi,⁵⁰ S. Suzuki,³⁹ S. Y. Suzuki,¹⁰ O. Tajima,¹⁰
 F. Takasaki,¹⁰ K. Tamai,¹⁰ N. Tamura,³² K. Tanabe,⁴⁸ M. Tanaka,¹⁰ G. N. Taylor,²³
 Y. Teramoto,³³ X. C. Tian,³⁶ S. Tokuda,²⁴ S. N. Tovey,²³ K. Trabelsi,⁹ T. Tsuboyama,¹⁰
 T. Tsukamoto,¹⁰ K. Uchida,⁹ S. Uehara,¹⁰ T. Uglov,¹⁴ K. Ueno,²⁹ Y. Unno,³ S. Uno,¹⁰
 Y. Ushiroda,¹⁰ G. Varner,⁹ K. E. Varvell,⁴³ S. Villa,²⁰ C. C. Wang,²⁹ C. H. Wang,²⁸
 J. G. Wang,⁵⁵ M.-Z. Wang,²⁹ M. Watanabe,³² Y. Watanabe,⁴⁹ L. Widhalm,¹³
 Q. L. Xie,¹² B. D. Yabsley,⁵⁵ A. Yamaguchi,⁴⁷ H. Yamamoto,⁴⁷ S. Yamamoto,⁵⁰
 T. Yamanaka,³⁴ Y. Yamashita,³¹ M. Yamauchi,¹⁰ Heyoung Yang,⁴¹ P. Yeh,²⁹ J. Ying,³⁶
 K. Yoshida,²⁴ Y. Yuan,¹² Y. Yusa,⁴⁷ H. Yuta,¹ S. L. Zang,¹² C. C. Zhang,¹² J. Zhang,¹⁰
 L. M. Zhang,⁴⁰ Z. P. Zhang,⁴⁰ V. Zhilich,² T. Ziegler,³⁷ D. Žontar,^{21,15} and D. Zürcher²⁰

(The Belle Collaboration)

¹*Aomori University, Aomori*

²*Budker Institute of Nuclear Physics, Novosibirsk*

³*Chiba University, Chiba*

⁴*Chonnam National University, Kwangju*

- ⁵*Chuo University, Tokyo*
- ⁶*University of Cincinnati, Cincinnati, Ohio 45221*
- ⁷*University of Frankfurt, Frankfurt*
- ⁸*Gyeongsang National University, Chinju*
- ⁹*University of Hawaii, Honolulu, Hawaii 96822*
- ¹⁰*High Energy Accelerator Research Organization (KEK), Tsukuba*
- ¹¹*Hiroshima Institute of Technology, Hiroshima*
- ¹²*Institute of High Energy Physics,
Chinese Academy of Sciences, Beijing*
- ¹³*Institute of High Energy Physics, Vienna*
- ¹⁴*Institute for Theoretical and Experimental Physics, Moscow*
- ¹⁵*J. Stefan Institute, Ljubljana*
- ¹⁶*Kanagawa University, Yokohama*
- ¹⁷*Korea University, Seoul*
- ¹⁸*Kyoto University, Kyoto*
- ¹⁹*Kyungpook National University, Taegu*
- ²⁰*Swiss Federal Institute of Technology of Lausanne, EPFL, Lausanne*
- ²¹*University of Ljubljana, Ljubljana*
- ²²*University of Maribor, Maribor*
- ²³*University of Melbourne, Victoria*
- ²⁴*Nagoya University, Nagoya*
- ²⁵*Nara Women's University, Nara*
- ²⁶*National Central University, Chung-li*
- ²⁷*National Kaohsiung Normal University, Kaohsiung*
- ²⁸*National United University, Miao Li*
- ²⁹*Department of Physics, National Taiwan University, Taipei*
- ³⁰*H. Niewodniczanski Institute of Nuclear Physics, Krakow*
- ³¹*Nihon Dental College, Niigata*
- ³²*Niigata University, Niigata*
- ³³*Osaka City University, Osaka*
- ³⁴*Osaka University, Osaka*
- ³⁵*Panjab University, Chandigarh*

³⁶*Peking University, Beijing*

³⁷*Princeton University, Princeton, New Jersey 08545*

³⁸*RIKEN BNL Research Center, Upton, New York 11973*

³⁹*Saga University, Saga*

⁴⁰*University of Science and Technology of China, Hefei*

⁴¹*Seoul National University, Seoul*

⁴²*Sungkyunkwan University, Suwon*

⁴³*University of Sydney, Sydney NSW*

⁴⁴*Tata Institute of Fundamental Research, Bombay*

⁴⁵*Toho University, Funabashi*

⁴⁶*Tohoku Gakuin University, Tagajo*

⁴⁷*Tohoku University, Sendai*

⁴⁸*Department of Physics, University of Tokyo, Tokyo*

⁴⁹*Tokyo Institute of Technology, Tokyo*

⁵⁰*Tokyo Metropolitan University, Tokyo*

⁵¹*Tokyo University of Agriculture and Technology, Tokyo*

⁵²*Toyama National College of Maritime Technology, Toyama*

⁵³*University of Tsukuba, Tsukuba*

⁵⁴*Utkal University, Bhubaneswer*

⁵⁵*Virginia Polytechnic Institute and State University, Blacksburg, Virginia 24061*

⁵⁶*Yonsei University, Seoul*

Abstract

We report the first observation of the radiative hyperonic B decay $B^+ \rightarrow p\bar{\Lambda}\gamma$, using a 140 fb^{-1} data sample recorded on the $\Upsilon(4S)$ resonance with the Belle detector at the KEKB asymmetric energy e^+e^- collider. The measured branching fraction is $\mathcal{B}(B^+ \rightarrow p\bar{\Lambda}\gamma) = (2.16_{-0.53}^{+0.58} \pm 0.20) \times 10^{-6}$. A search for $B^+ \rightarrow p\bar{\Sigma}^0\gamma$ yields no significant signal, so we set a 90% confidence-level upper limit on the branching fraction of $\mathcal{B}(B^+ \rightarrow p\bar{\Sigma}^0\gamma) < 3.3 \times 10^{-6}$.

PACS numbers: 13.40.Hq, 14.40.Nd, 14.20.Dh, 14.20.Jn

The $b \rightarrow s\gamma$ penguin diagram plays an essential role for the large rates of the observed radiative $B \rightarrow K^*\gamma$ [1] decays. It is also a good probe of new physics beyond the Standard Model [2]. Recently, the Belle collaboration reported a very stringent limit of $\mathcal{O}(10^{-6})$ on the branching fraction of two-body $B^+ \rightarrow p\bar{\Lambda}$ decays [3] but found an unexpectedly large rate for the three-body decay $B^0 \rightarrow p\bar{\Lambda}\pi^-$ [4], which proceeds presumably via the $b \rightarrow s$ penguin process. One interesting feature of the $B^0 \rightarrow p\bar{\Lambda}\pi^-$ decay is that the observed proton- $\bar{\Lambda}$ invariant mass $M_{p\bar{\Lambda}}$ spectrum peaks near threshold. Naively, a suppression of $\mathcal{O}(\alpha_{EM})$ is expected for the $B^+ \rightarrow p\bar{\Lambda}\gamma$ decay relative to $B^+ \rightarrow p\bar{\Lambda}$ if the former process is bremsstrahlung-like. In contrast, the short-distance $b \rightarrow s\gamma$ contribution can lead naturally to a non-bremsstrahlung-like energetic photon spectrum and an enhancement of $M_{p\bar{\Lambda}}$ at low mass; the former distribution can be compared to the recently measured $b \rightarrow s\gamma$ inclusive photon energy spectrum [5]. These features motivate our study of $B^+ \rightarrow p\bar{\Lambda}\gamma$. Some theoretical predictions [6] for the branching fraction of $B^+ \rightarrow p\bar{\Lambda}\gamma$ are at the $10^{-7} - 10^{-6}$ level, which is in the sensitivity range of the B-factories.

We use a data sample of 152×10^6 $B\bar{B}$ pairs, corresponding to an integrated luminosity of 140 fb^{-1} , collected by the Belle detector at the KEKB [7] asymmetric energy e^+e^- collider. The Belle detector is a large-solid-angle magnetic spectrometer that consists of a three-layer silicon vertex detector (SVD), a 50-layer central drift chamber (CDC), an array of aerogel threshold Čerenkov counters (ACC), a barrel-like arrangement of time-of-flight scintillation counters (TOF), and an electromagnetic calorimeter (ECL) comprised of CsI(Tl) crystals located inside a super-conducting solenoid coil that provides a 1.5 T magnetic field. An iron flux-return located outside of the coil is instrumented to detect K_L^0 mesons and to identify muons. The detector is described in detail elsewhere [8].

To identify the charged tracks, the proton (L_p), pion (L_π) and kaon (L_K) likelihoods are determined from the information obtained by the tracking system (SVD+CDC) and the hadron identification system (CDC+ACC+TOF). Prompt proton candidates must satisfy the requirements of $L_p/(L_p + L_K) > 0.6$ and $L_p/(L_p + L_\pi) > 0.6$, and not be associated with the decay of a Λ baryon. The prompt proton candidates are also required to satisfy track quality criteria based on the track impact parameters relative to the interaction point (IP). The deviations from the IP position are required to be within 0.3 cm in the transverse (x - y) plane, and within ± 3 cm in the z direction, where the z axis is opposite the direction of the positron beam. Candidate Λ baryons are reconstructed from two oppositely charged tracks,

one treated as a proton and the other as a pion, and must have an invariant mass within 5σ of the nominal Λ mass, as well as a displaced vertex and flight direction consistent with a Λ originating from the interaction point. To reduce background, a $L_p/(L_p + L_\pi) > 0.6$ requirement is applied to the proton-like track. Photon candidates are selected from the neutral clusters within the barrel ECL (with polar angle between 33° and 128°) having energy greater than 500 MeV. We discard any photon candidate if the invariant mass, in combination with any other photon above 30 (200) MeV, is within ± 18 (± 32) MeV/ c^2 of the nominal mass of the π^0 (η) meson. The above selection criteria are optimized using Monte Carlo (MC) simulated event samples.

Candidate B mesons are formed by combining a proton with a $\bar{\Lambda}$ and a photon [9], each defined using the above criteria, and requiring the beam-energy constrained mass, $M_{bc} = \sqrt{E_{\text{beam}}^2 - p_B^2}$, and the energy difference, $\Delta E = E_B - E_{\text{beam}}$, to lie in the ranges $5.2 \text{ GeV}/c^2 < M_{bc} < 5.29 \text{ GeV}/c^2$ and $-0.2 \text{ GeV} < \Delta E < 0.5 \text{ GeV}$. Here, p_B and E_B refer to the momentum and energy, respectively, of the reconstructed B meson, and E_{beam} refers to the beam energy, all in the $\Upsilon(4S)$ rest frame.

The dominant background is from continuum $e^+e^- \rightarrow q\bar{q}$ processes (where $q = u, d, s, c$) while the background from B decays is negligible except for possible feed-down events from $B^+ \rightarrow p\bar{\Sigma}^0\gamma$. This is confirmed with an off-resonance data set (10 fb^{-1}) accumulated at an energy that is 60 MeV below the $\Upsilon(4S)$, and an MC sample of 120 million continuum events. In the $\Upsilon(4S)$ rest frame, continuum events are jet-like while $B\bar{B}$ events are spherical. We follow the scheme defined in Ref. [10] and combine seven shape variables to form a Fisher discriminant [11] in order to maximize the distinction between continuum processes and signal. The variables used have almost no correlation with M_{bc} and ΔE . Probability density functions (PDFs) for the Fisher discriminant and the cosine of the angle between the B flight direction and the beam direction in the $\Upsilon(4S)$ frame are combined to form the signal (background) likelihood \mathcal{L}_s (\mathcal{L}_b). We require the likelihood ratio $\mathcal{R} = \mathcal{L}_s/(\mathcal{L}_s + \mathcal{L}_b)$ to be greater than 0.75; this suppresses about 86% of the background while retaining 78% of the signal. The selection point is determined by optimizing $N_s/\sqrt{N_s + N_b}$, where N_s and N_b denote the number of signal and background; here a signal branching fraction of 4×10^{-6} is assumed.

We perform an unbinned extended maximum likelihood fit to the events with $-0.2 \text{ GeV} < \Delta E < 0.5 \text{ GeV}$ and $M_{bc} > 5.2 \text{ GeV}/c^2$ to determine the signal yields. The extended

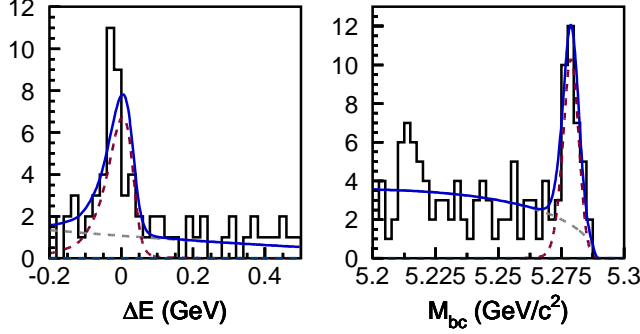


FIG. 1: The distributions of ΔE (for $M_{bc} > 5.27 \text{ GeV}/c^2$) and M_{bc} (for $-0.135 \text{ GeV} < \Delta E < 0.074 \text{ GeV}$) for $B^0 \rightarrow p\bar{\Lambda}\gamma$ candidates having $M_{p\bar{\Lambda}} < 2.4 \text{ GeV}/c^2$. The solid, dotted and dashed lines represent the combined fit result, fitted background and fitted signal, respectively.

likelihood function is defined as

$$\mathcal{L} = \frac{e^{-(N_\Lambda + N_\Sigma + N_{q\bar{q}})}}{N!} \prod_{i=1}^N \left[N_\Lambda P_\Lambda(M_{bc_i}, \Delta E_i) + N_\Sigma P_\Sigma(M_{bc_i}, \Delta E_i) + N_{q\bar{q}} P_{q\bar{q}}(M_{bc_i}, \Delta E_i) \right],$$

where P_Λ , P_Σ , and $P_{q\bar{q}}$ are the PDFs for $p\bar{\Lambda}\gamma$, $p\bar{\Sigma}^0\gamma$, and continuum background, respectively, and N_Λ , N_Σ , and $N_{q\bar{q}}$ are the corresponding number of candidates.

The $p\bar{\Lambda}\gamma$ and $p\bar{\Sigma}^0\gamma$ PDFs are two-dimensional smooth histograms determined by MC simulation. We use the parametrization first suggested by the ARGUS collaboration [12], $f(M_{bc}) \propto M_{bc} \sqrt{1 - (M_{bc}/E_{\text{beam}})^2} \exp[-\xi(1 - (M_{bc}/E_{\text{beam}})^2)]$, to model the background M_{bc} distribution and a quadratic polynomial for the background ΔE shape. We perform a two-dimensional unbinned fit to the ΔE vs M_{bc} distribution, with the signal and background normalizations as well as the continuum background shape parameters allowed to float.

The ΔE distribution (with $M_{bc} > 5.27 \text{ GeV}/c^2$) and the M_{bc} distribution (with $-0.135 \text{ GeV} < \Delta E < 0.074 \text{ GeV}$) for the region $M_{p\bar{\Lambda}} < 2.4 \text{ GeV}/c^2$ are shown in Fig. 1 along with the projections of the fit. The two-dimensional unbinned fit gives a $B^+ \rightarrow p\bar{\Lambda}\gamma$ signal yield of $34.1_{-6.6}^{+7.1}$ with a statistical significance of 8.6 standard deviations and a $B^+ \rightarrow p\bar{\Sigma}^0\gamma$ yield of 0.0 ± 4.7 . The significance is defined as $\sqrt{-2\ln(L_0/L_{\text{max}})}$, where L_0 and L_{max} are the likelihood values returned by the fit with signal yield fixed at zero and its best fit value, respectively [13].

We measure the differential branching fraction of $p\bar{\Lambda}\gamma$ by fitting the yield in bins of $M_{p\bar{\Lambda}}$, as shown in Fig. 2, and correcting for the corresponding detection efficiency as determined

from a large MC sample of events distributed uniformly in phase space. The results of the fits along with the efficiencies and the partial branching fractions are given in Table I. (In these fits, the signal yields are constrained to be non-negative.) The observed mass distribution in Fig. 2 peaks at low $p\bar{\Lambda}$ mass, a feature seen also in $B^0 \rightarrow p\bar{\Lambda}\pi^-$ and $B^+ \rightarrow p\bar{p}K^+$ decays [4, 14].

The photon energy spectrum in the $\Upsilon(4S)$ rest frame is measured using the same fit procedure and is shown in Fig. 3. The predicted shape for the generic $b \rightarrow s\gamma$ process, obtained by MC simulation, is shown in Fig. 3 as the shaded histogram. The two distributions agree with each other within the statistical uncertainty of the present measurement, although the mean of the $p\bar{\Lambda}\gamma$ spectrum is slightly higher.

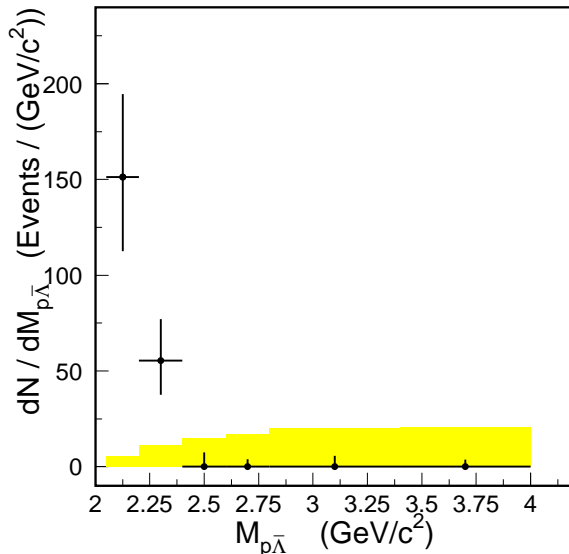


FIG. 2: The differential yield for $B^0 \rightarrow p\bar{\Lambda}\gamma$ as a function of $M_{p\bar{\Lambda}}$. The shaded distribution is from a phase-space MC simulation with area scaled to the observed signal yield.

We also study the proton angular distribution of the baryon pair system for $M_{p\bar{\Lambda}} < 4.0$ GeV/c^2 . The angle θ_X is measured between the proton direction and the γ direction in the baryon pair rest frame. Fig. 4 shows the efficiency corrected B yield in bins of $\cos\theta_X$. This distribution confirms the $b \rightarrow s\gamma$ fragmentation picture where the Λ tends to emerge opposite the direction of the photon.

The systematic uncertainty in particle selection is studied using high statistics control

TABLE I: The event yield, efficiency, and branching fraction (\mathcal{B}) for each $M_{p\bar{\Lambda}}$ bin.

$M_{p\bar{\Lambda}}$ (GeV/ c^2)	Signal Yield	Efficiency(%)	\mathcal{B} (10^{-6})
< 2.2	$22.7^{+6.5}_{-5.8}$	10.6	$1.41^{+0.40}_{-0.36}$
$2.2 - 2.4$	$11.1^{+4.3}_{-3.6}$	9.8	$0.74^{+0.29}_{-0.24}$
$2.4 - 2.6$	$0.0^{+1.5}_{-1.5}$	9.3	$0.00^{+0.11}_{-0.11}$
$2.6 - 2.8$	$0.0^{+0.8}_{-0.8}$	9.9	$0.00^{+0.06}_{-0.06}$
$2.8 - 3.4$	$0.0^{+3.4}_{-3.4}$	9.6	$0.00^{+0.23}_{-0.23}$
$3.4 - 4.0$	$0.0^{+2.2}_{-2.2}$	9.6	$0.00^{+0.15}_{-0.15}$
Total	$33.8^{+9.0}_{-8.1}$	-	$2.16^{+0.58}_{-0.53}$

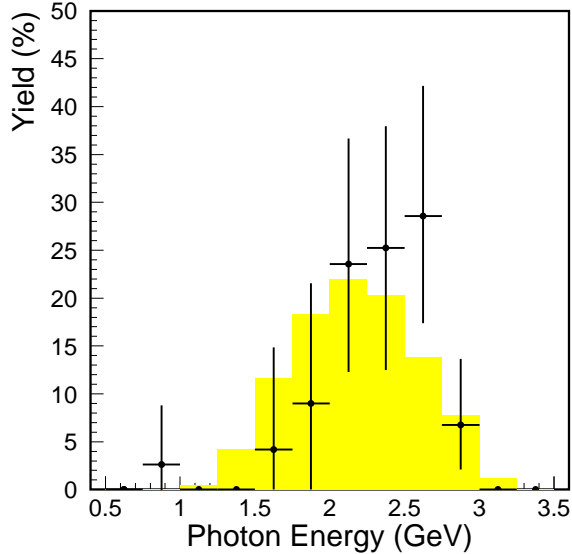


FIG. 3: Signal yield fraction versus photon energy in the $\Upsilon(4S)$ rest frame. The shaded histogram is the prediction from the inclusive $b \rightarrow s\gamma$ MC simulation.

samples. Proton identification is studied with a $\Lambda \rightarrow p\pi^-$ sample. The tracking efficiency is studied with a D^* sample, using both full and partial reconstruction. Based on these studies, we sum the correlated errors linearly and assign a 4.1% error for proton identification and 4.9% for the tracking efficiency.

For Λ reconstruction, we have an additional uncertainty of 2.5% on the efficiency for

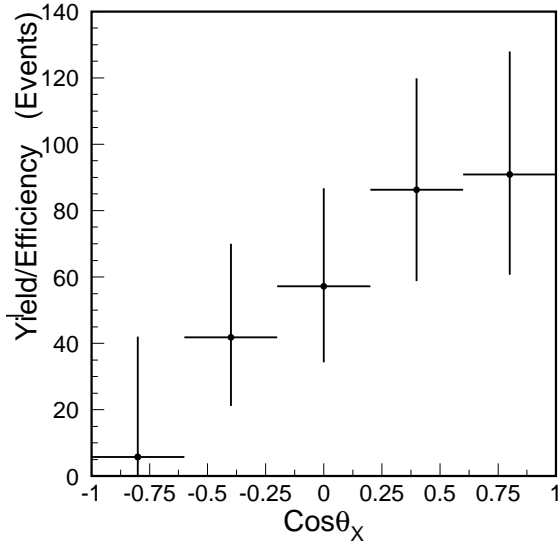


FIG. 4: Differential branching fraction versus $\cos\theta_X$ in the baryon pair system.

off-IP track reconstruction, determined from the difference of Λ proper time distributions for data and MC simulation. There is also a 1.2% error associated with the Λ mass selection and a 0.5% error for the Λ vertex selection [3]. Summing the errors for Λ reconstruction, we obtain a systematic error of 2.8%.

The 2.2% uncertainty for the photon detection is determined from radiative Bhabha events. For the π^0 and η vetoes, we compare the fit results with and without the vetoes; the difference of the branching fraction amounts to 0.5%, and we quote this as the associated systematic error.

Continuum suppression is studied by changing the selection criteria on \mathcal{R} in the interval 0 – 0.9 to see if there is any systematic trend in the signal fit yield. We quote a 2.5% error for this.

The systematic uncertainty from fitting is 2.2%, which is determined by varying the parameters of the signal and background PDFs by $\pm 1\sigma$. The MC statistical uncertainty and modeling with six $M_{p\bar{\Lambda}}$ bins contributes a 4.4% error (obtained by changing the $M_{p\bar{\Lambda}}$ bin size). The error on the number of total $B\bar{B}$ pairs is 0.7%. The error from the sub-decay branching fraction of $\Lambda \rightarrow p\pi^-$ is 0.8% [13].

We combine the above uncorrelated errors in quadrature. The total systematic error is 9.2%.

We see no evidence for the decay $B^+ \rightarrow p\bar{\Sigma}^0\gamma$. We use the fit results to estimate the expected background, and compare this with the observed number of events in the $p\bar{\Sigma}^0\gamma$ signal region ($-0.20 \text{ GeV} < \Delta E < 0.04 \text{ GeV}$ and $M_{bc} > 5.27 \text{ GeV}/c^2$) in order to set an upper limit on the yield [15, 16, 17]. The estimated background for $M_{p\bar{\Lambda}} < 2.4 \text{ GeV}/c^2$ ($M_{p\bar{\Lambda}} < 4 \text{ GeV}/c^2$) is $45.5 \pm 6.3(84 \pm 0.2)$, the number of observed events is 44 (96), and the systematic uncertainty is 9.2%; from these, the upper limit yield is 14.9 (35.5) at 90% confidence level. The efficiency, estimated from the phase space MC simulation, is 12.1% (7.0%), so the 90% confidence-level upper limits for the branching fractions are $\mathcal{B}(B^0 \rightarrow p\bar{\Sigma}^0\gamma) < 0.8 \times 10^{-6}$ for $M_{p\bar{\Lambda}} < 2.4 \text{ GeV}/c^2$ and $\mathcal{B}(B^0 \rightarrow p\bar{\Sigma}^0\gamma) < 3.3 \times 10^{-6}$ for $M_{p\bar{\Lambda}} < 4.0 \text{ GeV}/c^2$.

In summary, we have performed a search for the radiative baryonic decays $B^0 \rightarrow p\bar{\Lambda}\gamma$, and $p\bar{\Sigma}^0\gamma$ with 152 million $B\bar{B}$ events. A clear signal is seen in the $p\bar{\Lambda}\gamma$ mode, and we measure a branching fraction of $\mathcal{B}(B^+ \rightarrow p\bar{\Lambda}\gamma) = (2.16_{-0.53}^{+0.58} \text{ (stat)} \pm 0.20 \text{ (syst)}) \times 10^{-6}$, which is consistent with the upper limit set by CLEO[18]. The yield of the $B^0 \rightarrow p\bar{\Sigma}^0\gamma$ mode is not statistically significant, and we set the 90% confidence level upper limit of $\mathcal{B}(B^0 \rightarrow p\bar{\Sigma}^0\gamma) < 3.3 \times 10^{-6}$ for $M_{p\bar{\Lambda}} < 4.0 \text{ GeV}/c^2$.

We thank the KEKB group for the excellent operation of the accelerator, the KEK Cryogenics group for the efficient operation of the solenoid, and the KEK computer group and the NII for valuable computing and Super-SINET network support. We acknowledge support from MEXT and JSPS (Japan); ARC and DEST (Australia); NSFC (contract No. 10175071, China); DST (India); the BK21 program of MOEHRD and the CHEP SRC program of KOSEF (Korea); KBN (contract No. 2P03B 01324, Poland); MIST (Russia); MESS (Slovenia); NSC and MOE (Taiwan); and DOE (USA).

* on leave from Nova Gorica Polytechnic, Nova Gorica

- [1] R. Ammar *et al.* (CLEO Collaboration), Phys. Rev. Lett. **71**, 674 (1993); B. Aubert *et al.* (BaBar Collaboration), Phys. Rev. Lett. **88**, 101805 (2002); M. Nakao, et al. (Belle Collaboration), Phys. Rev. D **69**, 112001 (2004)
- [2] T. Hurth, E. Lunghi and W. Porod, hep-ph/0312260 and references therein.
- [3] K. Abe *et al.* (Belle Collaboration), Phys. Rev. D **65**, 091103 (2002).
- [4] M.-Z. Wang, *et al.* [Belle Collaboration], Phys. Rev. Lett. **90**, 201802 (2003)

- [5] P.Koppenburg, *et al.* (Belle Collaboration), hep-ex/0403004.
- [6] H.Y. Cheng, Phys. Lett. B 533 (2002); C.Q. Geng and Y.K. Hsiao hep-ph/0405283.
- [7] S. Kurokawa and E. Kikutani *et al.*, Nucl. Instr. and Meth. A **499**, 1 (2003).
- [8] A. Abashian *et al.* (Belle Collaboration), Nucl. Instr. and Meth. A **479**, 117 (2002).
- [9] Throughout this report, inclusion of charge conjugate mode is always implied unless otherwise stated.
- [10] K. Abe *et al.* (Belle Collaboration), Phys. Lett. **B517**, 309 (2001).
- [11] R.A. Fisher, Annals of Eugenics **7**, 179 (1936).
- [12] H. Albrecht *et al.*, Phys. Lett. **B241**, 278 (1990); *ibid.* **B254**, 288 (1991).
- [13] K. Hagiwara *et al.* (Particle Data Group), Phys. Rev. D **66**, 010001 (2002).
- [14] M.Z. Wang *et al.* (Belle Collaboration), Phys. Rev. Lett.**92**, 131801 (2004).
- [15] R.D. Cousins and V.L. Highland, Nucl. Instr. and Meth. A **320**, 331 (1993).
- [16] G.J. Feldman and R.D. Cousins, Phys. Rev. D **57**, 3873 (1998).
- [17] J. Conrad *et al.*, Phys. Rev. D **67**, 012002 (2003).
- [18] K. W. Edwards *et al.* [CLEO Collaboration], Phys. Rev. D **68**, 011102 (2003) .